UCRL-ID-123633

PCMDI
Program for Climate Model Diagnosis and Intercomparison

PCMDI Report No. 33

MODEL SIMULATED NORTHERN WINTER CYCLONE AND ANTICYCLONE ACTIVITY UNDER A GREENHOUSE WARMING SCENARIO

by

Yi Zhang[1] and Wei-Chyung Wang[2]

[1]Program for Climate Model Diagnosis and Intercomparison
Lawrence Livermore National Laboratory, Livermore, CA, USA

[2]Atmospheric Science Research Center
State University of New York at Albany, Albany, NY, USA

March 1996

PROGRAM FOR CLIMATE MODEL DIAGNOSIS AND INTERCOMPARISON
UNIVERSITY OF CALIFORNIA, LAWRENCE LIVERMORE NATIONAL LABORATORY
LIVERMORE, CA 94550

ABSTRACT

Two one-hundred-year equilibrium simulations from the NCAR Community Climate Model (CCM1) are used to investigate the activity of northern winter extratropical cyclones and anticyclones under normal and greenhouse warming climate conditions. The first simulation uses the 1990 observed CO_2, CH_4, N_2O, CFC-11 and CFC-12 concentrations and the second adopts the year 2050 concentrations according to the IPCC business-as-usual scenario. Variables that describe the characteristic properties of the cyclone-scale eddies, such as surface cyclone and anticyclone frequency and band-passed root-mean-square (RMS) of 500 hPa geopotential height, along with the Eady growth rate maximum, form a framework for the analysis of the cyclone and anticyclone activity.

Objective criteria are developed for identifying cyclone and anticyclone occurrence based on the 1000 hPa geopotential height and vorticity fields and tested using ECMWF analyses. The potential changes of the eddy activity under the greenhouse warming climate were then examined. Results indicate that the activity of cyclone-scale eddies decreases under the greenhouse warming scenario. This is not only reflected in the surface cyclone and anticyclone frequency and the band-passed RMS of 500 hPa geopotential height, but is also discerned from the Eady growth rate maximum. Based on the analysis, three different physical mechanisms responsible for the decreased eddy activity are discussed: (1) decrease of the extratropical meridional temperature gradient from surface to mid-troposphere; (2) reduction in the land-sea thermal contrast in the east coastal regions of the Asian and North American continents; and (3) increase in the eddy meridional latent heat fluxes. Uncertainties of the results related to the limitations of the model and the model equilibrium simulations are discussed.

1. Introduction

The passage of extratropical cyclones and anticyclones is closely linked to the day-to-day weather changes and local climate in the mid-latitudes. These cyclone-scale eddies play an important role in transporting heat, momentum and moisture in the extratropical regions and are an indispensable part of the general circulation of the atmosphere (Newton, 1969). Study of the long-term variation of extratropical cyclone and anticyclone activity is thus essential for the understanding of extratropical climate change.

Although extensive research has greatly improved our understanding on nearly all aspects of the extratropical cyclones and anticyclones (Newton and Holopainen, 1990), our knowledge of the long-term climatology of cyclones and anticyclones is still very limited. The most often cited work on this subject are still those of Petterssen (1956) and Klein (1957). And almost all of the studies in this area to date have been devoted to documenting the observed long-term variations of cyclone and anticyclone frequency and intensity, although the physical mechanisms that affect the variations of the long-term cyclone-scale eddy activity are not well understood. For example, the cause of the drastic decrease in cyclone and anticyclone frequency from the 1950s to the 1970s in North America as documented by Zishka and Smith (1980) and Whittaker and Horn (1981) is still a mystery.

The long-term variation in cyclone and anticyclone activity is known to be important to the general circulation of the atmosphere and is related to the global radiation balance because the heat transported by these eddies dominates the total atmospheric energy transport in the mid-latitudes (Holopainen, 1965). The global radiation balance can be disturbed by many factors, typically the increases in atmospheric greenhouse gas concentration and aerosol loadings. In this study, the response of cyclone and anticyclone activity to a global radiative perturbation will be examined by investigating eddy activity under the greenhouse warming scenario. To achieve this goal, relevant interacting physical processes in the climate system have to be considered. General Circulation Models (GCMs), which have long been recognized as the best available means to consider simultaneously the wide range of interacting physical processes that characterize the climate system, will be used in this study.

There have been several GCM studies related to the cyclone and anticyclone activity under increased CO_2 conditions. Konig et al. (1993), based on analysis of model simulated northern hemisphere surface cyclone frequency, suggested that there is no significant difference in cyclone

frequency between the greenhouse warming and normal climate conditions. More recently, Lambert (1995) indicated, using the Canadian Climate Centre model, that the total number of northern hemisphere winter cyclones decreased and the frequency of intense cyclones increased under 2 x CO_2 conditions.

Both studies have addressed the important issue of the possible changes in the activity of cyclone-scale eddies under the greenhouse warming condition. Differences in the conclusions from the studies may stem from using different methods in approaching the problem and the model dependence of the results. These studies could also have adopted a more complete set of variables. For example, the only quantity used in Konig et al. (1993) was cyclone frequency at 1000 hPa; Lambert (1995) also focused on the surface cyclone frequency and intensity. Because the extratropical cyclones and anticyclones are baroclinic disturbances and they extend from the surface to middle and upper troposphere, a better approach is to study both the surface and the 500 hPa fields so that these eddies can be examined three-dimensionally. More importantly, none of the studies has adequately addressed the physical mechanisms that caused the changes in cyclone and anticyclone activity under the warming climate.

In order to better understand the cyclone and anticyclone activity under the greenhouse warming scenario, we will approach this problem more comprehensively than Lambert (1995) and Konig et al. (1993). Cyclone-scale eddy activity will be examined by using both the surface and 500 hPa quantities as well as a quantity that relates to the basic flow baroclinicity. In addition, we will emphasize physical mechanisms that cause changes in cyclone and anticyclone activity under the warming scenario.

Historically, cyclones have been the focus of most studies since they are often associated with precipitation and stormy weather. It is actually more appropriate to include both cyclones and anticyclones, because the atmospheric variability and weather changes arise from the vorticity advection, which is related to the movement of both cyclones and anticyclones. Thus, the variables chosen for this study includes: (1) variables that describe the basic characteristics of both cyclones and anticyclones, i.e., surface cyclone and anticyclone frequency and their geographical distribution, and the band-passed (2.5-6 days) RMS of 500 hPa geopotential height; (2) Eady growth rate maximum (or baroclinic parameter), a variable that represents the basic flow baroclinicity. These two groups of quantities will serve as a framework to examine the cyclones and anticyclones and to determine whether these eddies become more or less active under the greenhouse warming

condition. Some of the variables will also be used to explain the physical mechanisms related to the changing eddy activity.

In section 2 we will briefly describe the model simulations and observational data. The design and testing of the objective criteria for identification of surface cyclones and anticyclones are discussed in section 3. The analysis of eddy activity under greenhouse warming conditions and the discussion of physical mechanisms are in section 4, and conclusions appear in section 5.

2. Model simulations and observational data

The model is based on version 1 of the National Center for Atmospheric Research (NCAR) Community Climate Model (CCM1), with incorporation of the radiative effects of trace gases (CH_4, N_2O, CFC-11, CFC-12). CCM1 is a spectral model with rhomboidal wavenumber 15 truncation. This truncation yields an effective grid resolution of 7.5° longitude and approximately 4.5° latitude. The model has 12 sigma levels in the vertical using energy-conserving vertical finite differences. Realistic land/ocean distributions and topography are used with the seasonal cycle included, and both large-scale condensation and moist convective adjustments are included in the cloud prediction schemes of the model. Major model characteristics such as circulation statistics, cloud radiative forcing and sensitivity of climate simulations to horizontal resolution have been extensively examined in many studies (see Kiehl and Williamson, 1991 and references therein). A detailed description of CCM1 can be found in Williamson et al. (1987). Two 100-year equilibrium simulations were performed (Wang et al., 1992) by coupling CCM1 with a 50-meter mixed-layer ocean model containing seasonal heat storage, the first with observed 1990 concentrations of CO_2 and trace gases and the second with increased concentrations of CO_2 and trace gases at the level of the year 2050 under the business-as-usual scenario of the IPCC (Houghton et al., 1990). Comparisons between the two cases provided the equilibrium climate changes due to projected increases of CO_2 and other trace gases between 1990 and 2050

Global and annual mean changes of some important climate variables for the two cases are l annual mean surface air temperature by 3.9°C. Consistent with this surface warming, the global averaged cloud cover decreases and the precipitation and moisture increase. These characteristics are similar to other GCM simulations on the greenhouse effect (Houghton et al., 1992). Also, the inclusion of other trace gases in the current model yields a more realistic simulation of the surface

and the upper troposphere temperature and humidity in the present climate than those that use CO_2 as a proxy (Wang et al.,1991).

Table 1: GCM simulated global and annual mean surface air temperature Ts (k), precipitation P (mm/day), cloud cover (%) and column water vapor Q (mm).

Case	Ts	dTs	P	dP	C	dC	Q	dQ
control	288.9	-----	3.39	-----	46.0	-----	25.5	-----
warming	292.9	3.88	3.64	0.25	44.6	-1.4	32.4	6.9

Observational data for testing the cyclone-searching criteria is from 10 years (1979-1988) of ECMWF December-February (DJF) initialized analysis. For consistency between the horizontal resolution of the model and the observations, the R15 version of the ECMWF analyses will be used for the testing. All the analyses and figures to be shown are for the northern hemisphere ten-year winter (DJF) seasonal average unless otherwise specified.

3. Criteria for identifying cyclones/anticyclones

A proper set of numerical criteria for identifying cyclones and anticyclones in the model is needed for this study. Considering the scale and characteristics of extratropical cyclones and anticyclones, the following criteria have been designed to identify cyclones/anticyclones in the extratropical regions (25°N to 70°N):

1) Minimum (maximum) 1000 hPa geopotential height at the grid point relative to the eight surrounding points is required.

2) Identified cyclonic (anticyclonic) vorticity at the grid point must remain at least 24 hours.

3) Relative vorticity magnitude at 1000 hPa must exceed a critical value of 2.0×10^{-5} s^{-1} (or 1.0×10^{-5} s^{-1}).

Disturbances satisfying the above criteria are defined as cyclones (anticyclones). Multi-counting of the same cyclone (anticyclone) at one grid point in adjacent time periods must be avoided because the criteria are applied to the data twice a day. To do this, we explicitly limit at most one cyclone/ anticyclone at one grid point within 48 hours. Due to the coarse resolution of the model, the representation of high terrain is quite crude. Computational biases arise in the vicinity of the Tibetan Plateau when the 1000 hPa fields are interpolated. Any points that are in the Plateau or within two

grid points of the Plateau are excluded from the counting. These identification criteria, similar to those of Konig et al. (1993) and Lambert (1988), use the minimum 1000 hPa geopotential height as the quantity for initial identification. Constraints on the magnitude and duration of the 1000 hPa vorticity field are then applied for further identification.

Based upon the above criteria, the cyclone events are counted for ten years (1979-1988) from the ECMWF observational analyses (shown in Fig. 1 (a)). Comparing the percentage frequency of cyclone centers from Petterssen (1956) in Fig. 1 (b), we find that the maximum cyclone frequency centers are remarkably close. The geographical location of the Pacific and the Atlantic cyclone centers are almost identical. The two plots also have very similar detailed regional characteristics in the northwestern Pacific where a tongue of cyclone frequency maximum extends southward along the west coast of North America. In the Atlantic, maximum frequency bands in both plots exhibit a marked southwest-northeast orientation. The maximum cyclone frequency in the vicinity of the Mediterranean is also correctly reproduced by these criteria. Fig. 2 is the same as Fig. 1 except for anticyclones. Compared with the cyclone centers in Fig. 1, the anticyclones occur at relatively lower latitude and their frequency bands extend more along latitude lines. In Fig. 2 (a), the orientation and the geographical position of the two bands of maximum anticyclone frequency are very close to those in Fig. 2 (b). The three high frequency centers at around 170°E-180°E, 130°W and 30°W agree well between the two plots. In general, the geographical locations of the surface cyclone and anticyclone frequency identified through these criteria agree well with their respective results from Petterssen (1956), although the quantitative comparison between the two is very difficult. This is because the frequency of cyclones and anticyclones is computed in terms of percentage frequency of every 100,000 km^2 in Petterssen's study, while the frequency is measured in real numbers in the current study. In order to quantitatively compare the current cyclone and anticyclone frequency distribution with those from the previous studies, we reconstructed Fig. 3, the northern winter seasonal mean (1958 -1977) cyclone frequency distribution based on the data from Whittaker and Horn (1982). As expected, the qualitative features of Fig. 3 are very similar to those from Fig. 1 (a) and Fig. 1 (b). In a quantitative sense, the Pacific and the Atlantic maximum frequency in Fig. 3 is typically around 10 to 12 every season, while the magnitude of the same quantity is about 8 to 10 from Fig. 1 (a). In rough terms, the cyclone numbers in the Pacific, the Atlantic and the Mediterranean from Fig. 1 (a) are about 2/3 ~ 3/4 of those from Fig. 3. Clearly, the

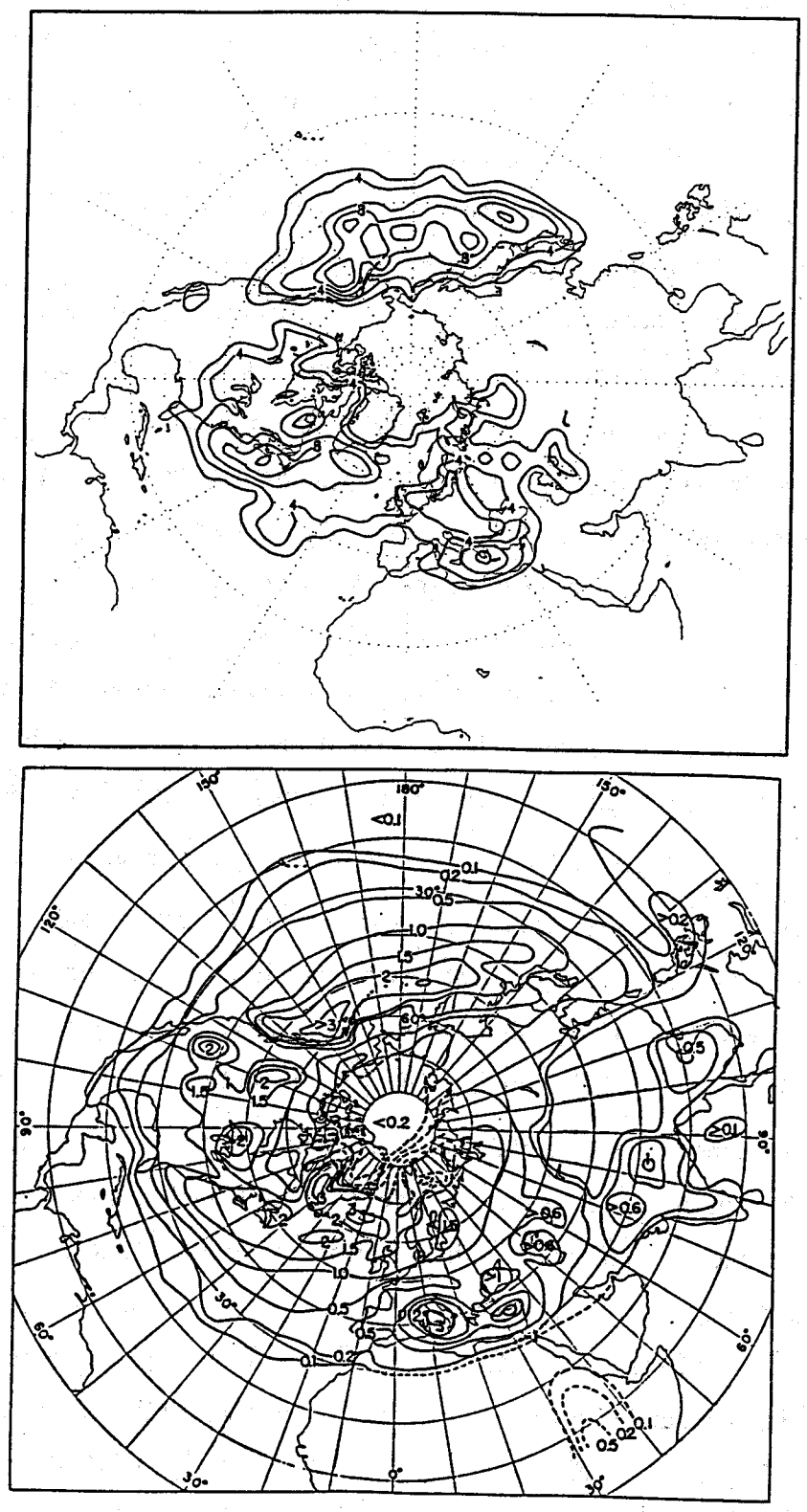

Fig. 1. (a) Winter seasonal averaged cyclone events from ECMWF global analyses (1979-1988) identified through the cyclone searching criteria. Unit: number of events. (b) Winter seasonal averaged percentage frequency of cyclone centers during 1899 to 1939 from Petterssen (1956). Unit: Percentage frequency per 100,000 km^2.

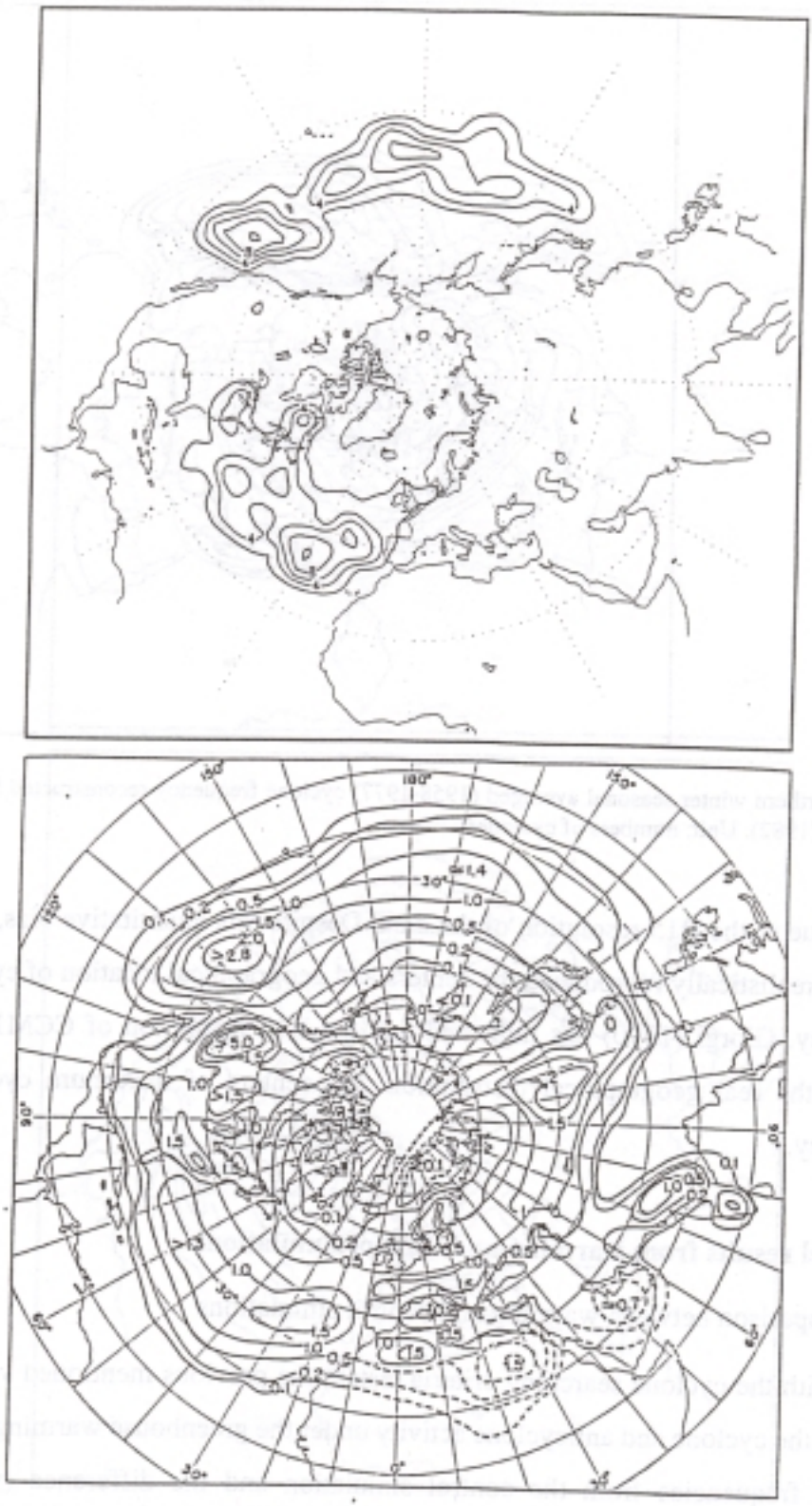

Fig. 2. (a) Same as in Fig. 1. (a) except for anticyclones. (b) Same as in Fig. 1. (b) except for anticyclones.

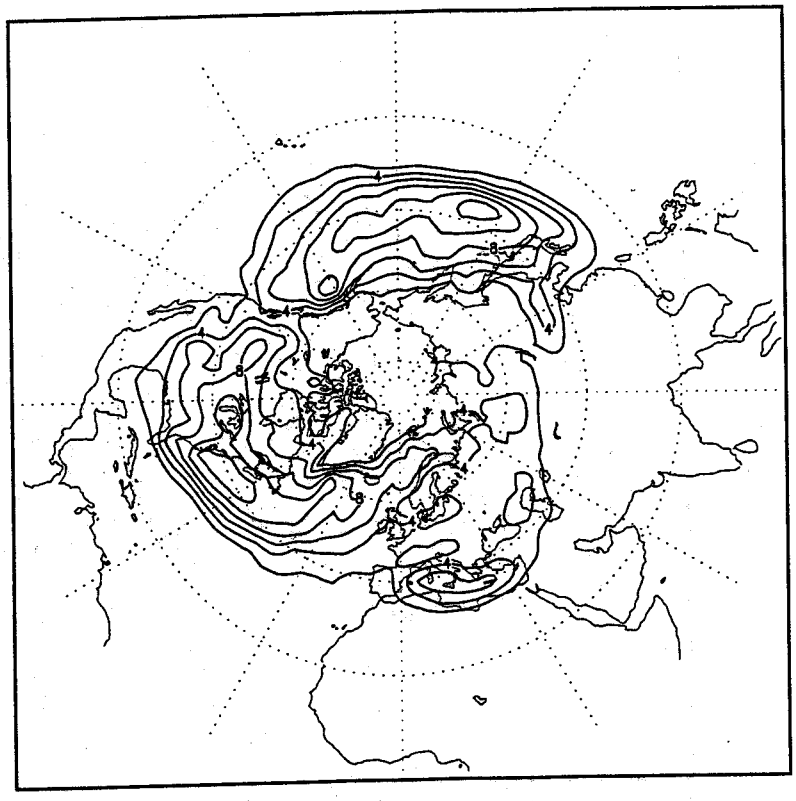

Fig. 3. Northern winter seasonal averaged (1958-1977) cyclone frequency reconstructed from the data of Whittaker and Horn (1982). Unit: numbers of cyclones.

bias is due to the R15 resolution of the data. Despite this quantitative bias, the R15 truncation of the data realistically reproduced the centers and geographical location of cyclone and anticyclone frequency. Giorgi (1990) has indicated that the R15 resolution of CCM1 can also realistically portray the real geographical distribution and centers of maximum cyclone and anticyclone frequency.

4. **Model results from warming and control simulations**

4.1 Comparison between warming and control simulations

With the cyclone searching criteria tested, the previous mentioned variables can be used to analyze the cyclone and anticyclone activity under the greenhouse warming scenario. Fig. 4 shows cyclone frequencies from the control simulation and the difference (warming - control) of frequencies between the warming and the control simulations. Although areas with both decreased and increased frequency can be found, the magnitude and areas of decreased frequency clearly

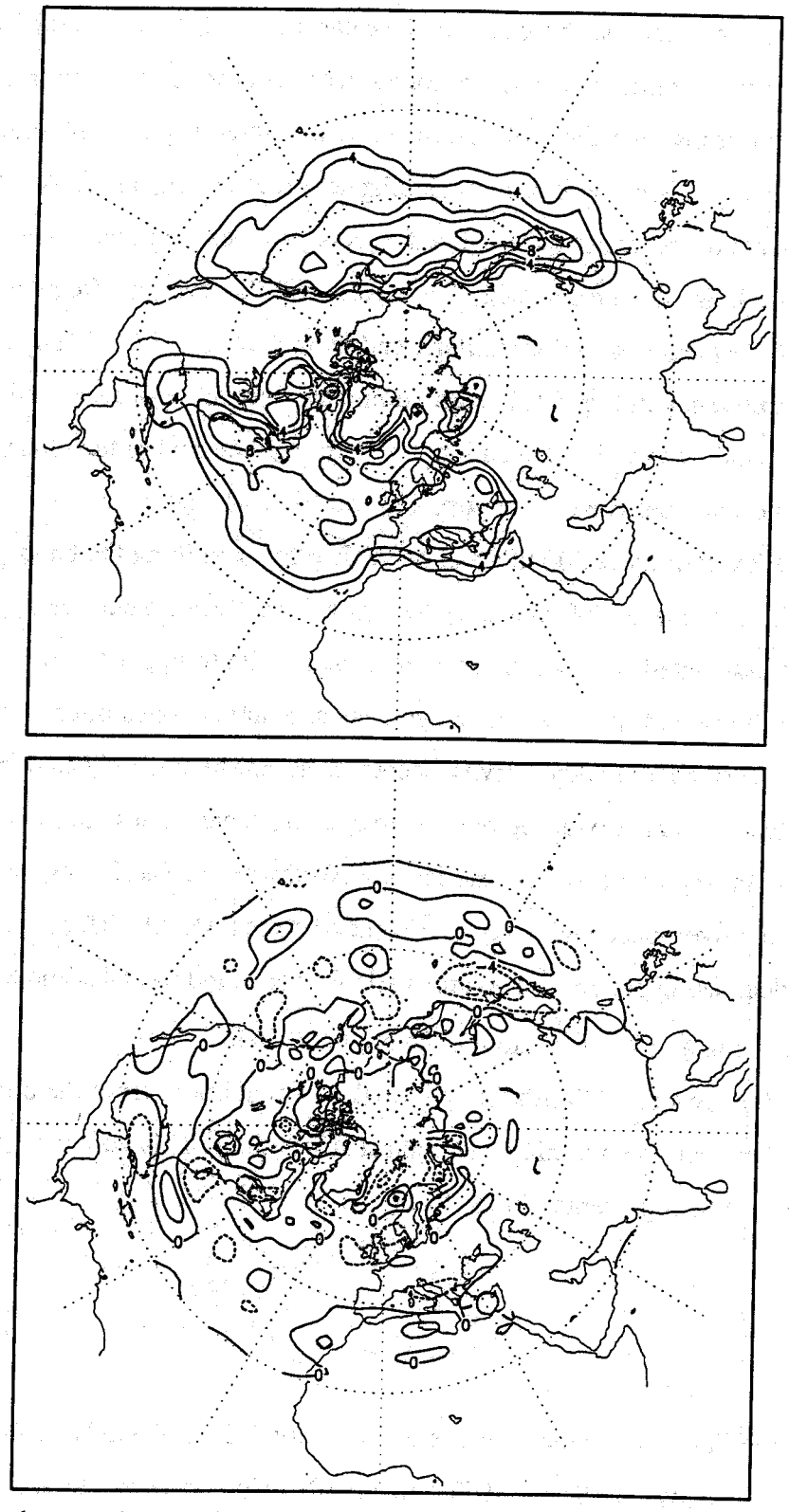

Fig. 4. (a) Winter seasonal averaged geographical distribution of cyclone frequency from the control simulation. Unit: numbers of events. (b) Difference of cyclone frequency between warming and control simulations. Units: numbers of events.

outnumber those of increased frequency. One particular interesting phenomenon is that three of the most prominent minimum centers are found near the east coast of North America, East Asia and surrounding oceans, and the Mediterranean. These three regions are among the most important cyclogenesis regions in the Northern Hemisphere (Petterssen, 1956; Whittaker and Horn, 1982). The significant decreases of the cyclone frequency in these regions suggest that the cyclongenesis has decreased. In agreement with the change of the cyclone frequency, the comparison of anticyclone frequency shows a similar trend as indicated in Fig. 5. The areas and magnitude of decreased frequency in Fig. 5 (b) clearly dominate over those of increased frequency. It should be noticed that the geographical locations of both cyclone and anticyclone frequency bands have remained the same between the control and warming simulations.

The eddy activity at 500 hPa can be studied by examining the band-pass filtered (period 2.5 - 6 days) RMS value of 500 hPa geopotential height. Because surface cyclones and anticyclones are always associated with wave patterns in the middle to upper troposphere, high values of this quantity are expected in areas where cyclones and anticyclones often occur. Consistent with the trend at the surface, the eddy activity decreases at 500 hPa as indicated in Fig. 6. The maximum reduction tends to occur over regions where cyclone-scale eddies are found most active, including the east coastal region of North America, the Northwestern Pacific region and the Mediterranean. The reduction over these regions is consistent with the trend of surface cyclones and anticyclones. A similar decreasing pattern of the same variable was found by Bates and Meehl (1985) in a $2xCO_2$ simulation using an earlier version of the NCAR CCM.

Fig. 7. shows the 780 hPa Eady growth rate maximum from the control simulation and the difference between the warming and control simulations. This variable, also called the baroclinic parameter, can be represented in the form

$$\sigma_{BI} = 0.31 f \left| \frac{\partial V}{\partial Z} \right| N^{-1}$$

where f is the Coriolis parameter, N is static stability, V is total wind and Z is height. This parameter was first shown by Lindzen and Farrell (1980) to be an accurate estimate of the growth rate maximum in a range of baroclinic instability problems. Hoskins and Valdes (1990) used this parameter as a measure of the basic flow baroclinicity and indicated that a proper way to determine

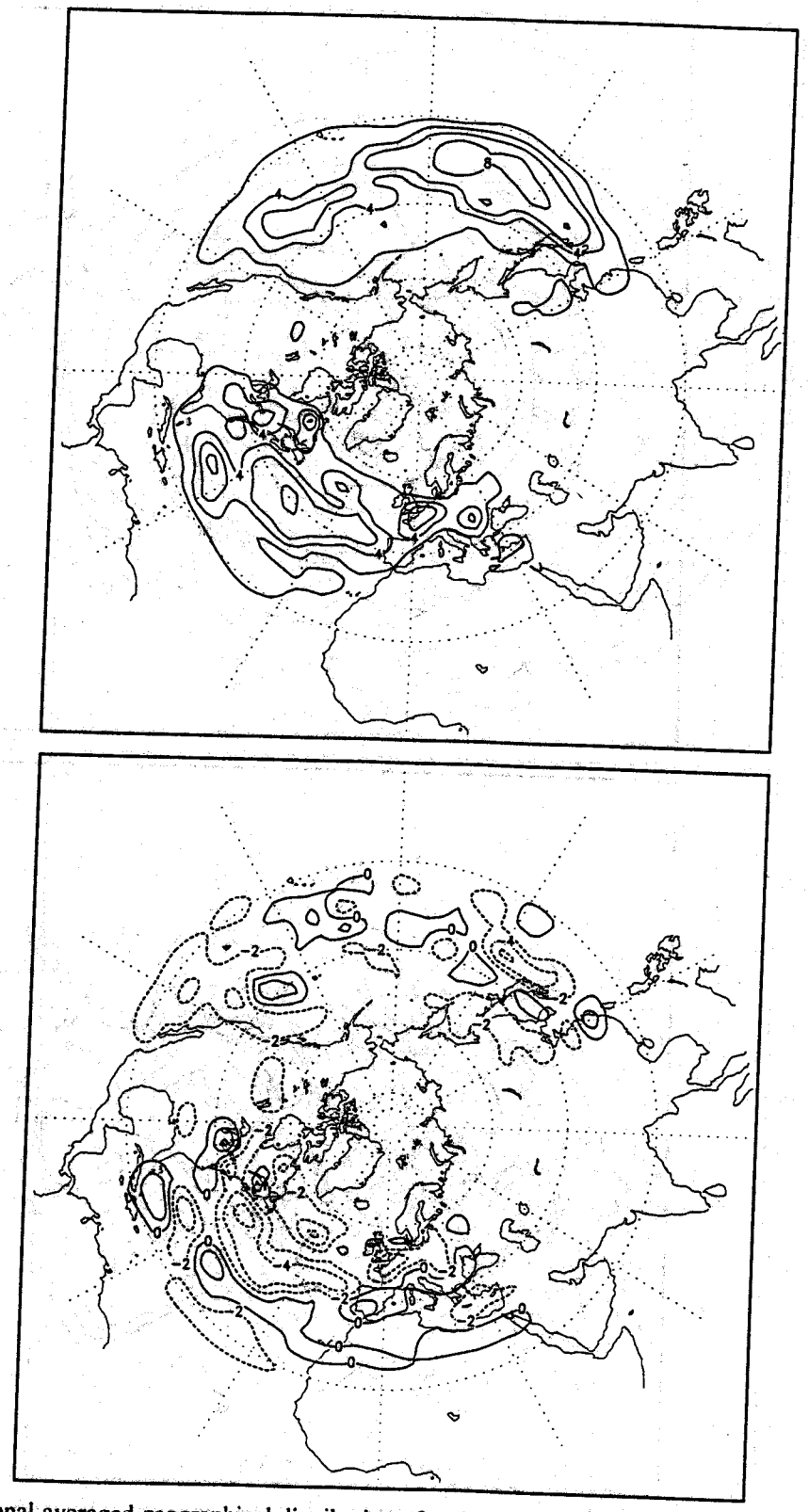

Fig. 5. (a) Winter seasonal averaged geographical distribution of anticyclone frequency from the control simulation. Unit: numbers of events. (b) Difference of anticyclone frequency between warming and control simulations. Unit: numbers of events.

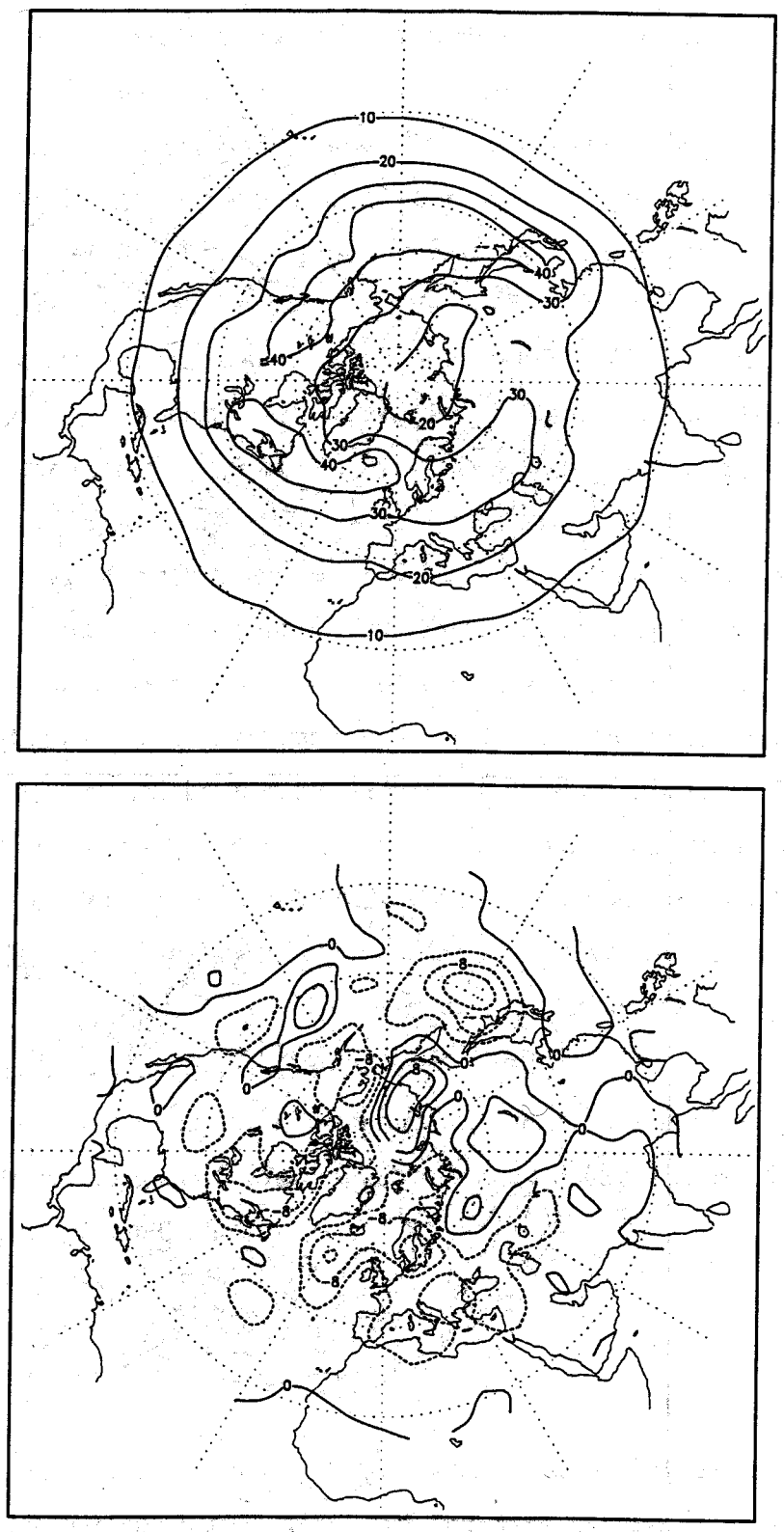

Fig. 6. (a) Winter seasonal averaged band-passed RMS of 500 hPa geopotential height from control simulation. Unit: meters. (b) Difference of RMS of 500 hPa geopotential height between the warming and control simulations. Unit: meters.

Fig. 7. (a) Winter seasonal averaged Eady growth rate maximum at 780 hPa from control simulation. Unit: day^{-1} (b) Difference of the Eady growth rate maximum between the warming and control simulations. Unit: day^{-1}

its value is to calculate above the boundary layer where N tends not to play a dominant role. The region in Fig. 7 where the 780 hPa level is within 1 km of the orography and probably in the boundary layer, is blocked. Clearly, a reduction of the atmospheric baroclinicity occurred in most areas of the mid-latitudes. The magnitude of the decrease in these areas ranges from 0 day^{-1} to 0.08 day^{-1}. If the mean baroclinicity and the Eady growth rate maximum are at all related to the extratropical baroclinic eddy activity, the reduction in its magnitude implies less active cyclone-scale eddies, which agrees with what has been discussed above.

4.2 Physical mechanisms

The analyses of the variables related to the extratropical cyclone-scale eddies in the previous section have consistently indicated that the eddy activity decreases under the greenhouse warming scenario. In this section, we discuss the physical mechanisms that are responsible for the decrease.

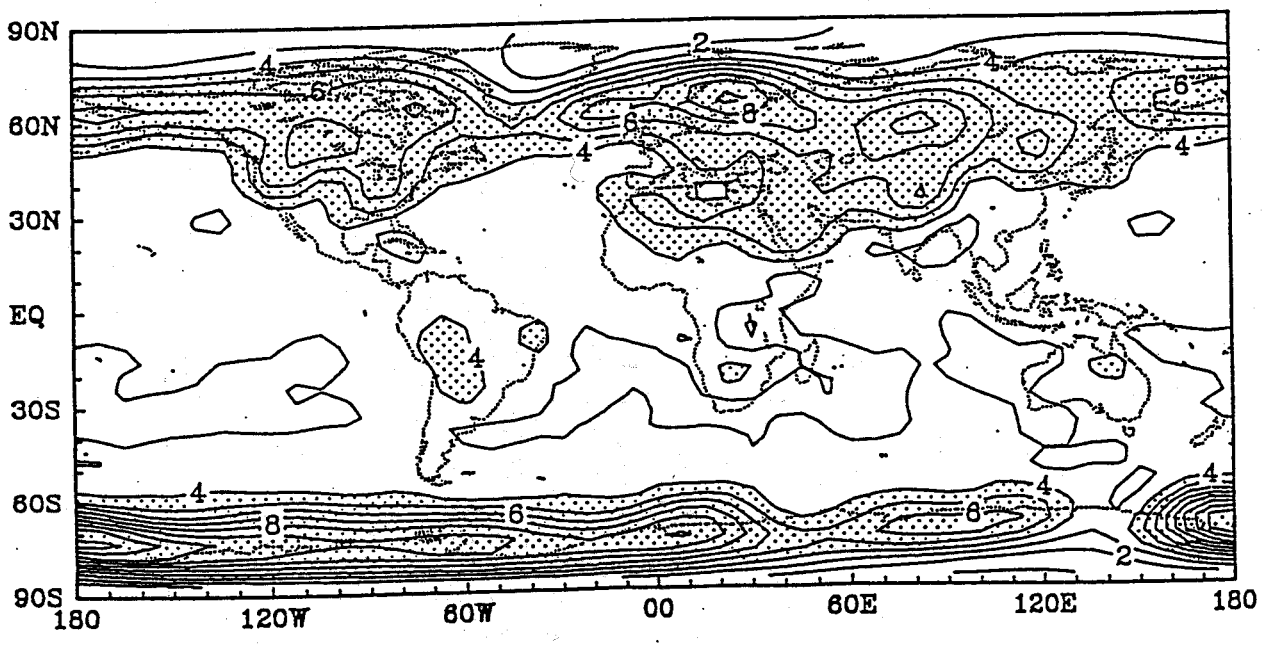

Fig. 8. Difference of the winter seasonal averaged surface air temperature between warming and control simulations. Areas with warming greater than 4°C are shaded. Unit: °C

The difference in surface air temperature between the two simulations is plotted in Fig. 8. Note that the large magnitude of warming occurs primarily north of 55°N, a consistent feature from all models due to the feedback between temperature and snow-ice albedo (Mitchell et al., 1990).

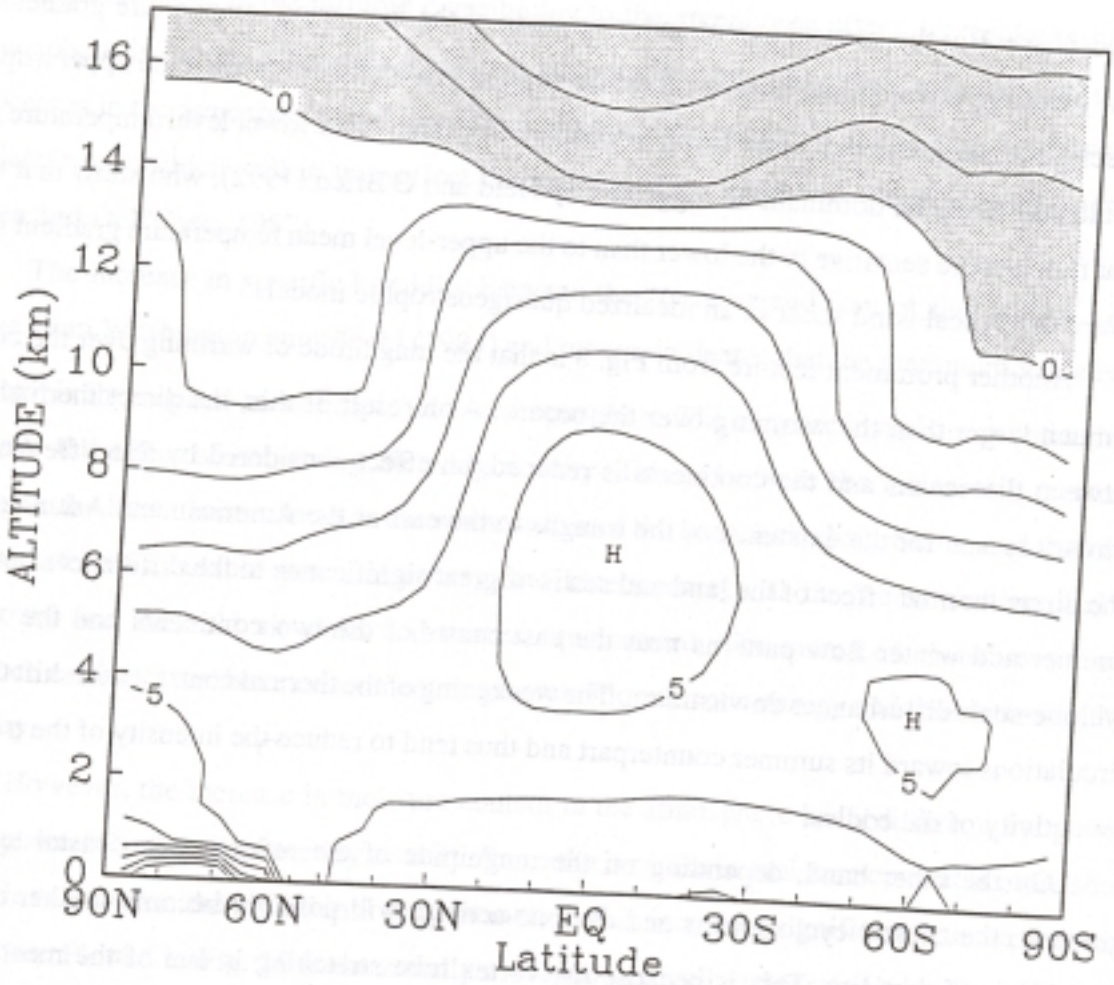

Fig. 9. Zonal mean vertical distribution of temperature difference between warming and control simulation. Unit: °C

The nonuniform warming pattern means weaker meridional surface air temperature gradient in the extratropical region. Because the baroclinicity of the flow and the strength of the cyclone-scale eddies are inherently related to the meridional temperature gradient throughout the troposphere, the reduction of the surface temperature gradient alone does not necessarily mean the weakening of the mean flow baroclinicity. Plotted in Fig. 9 is the zonally averaged vertical distribution of temperature difference between the two simulations. There is a very strong temperature increase north of 60°N and below 2 km, and decreasing temperature gradient in the extratropics up to 5 km. Clearly, a reduction in temperature gradient of such depth will weaken the atmospheric mean flow baroclinicity. A slight increase in temperature gradient occurs above 5 km. This increase in the upper troposphere may slightly offset the effect of the decreasing temperature in the lower

troposphere. But the vertical extent and magnitude of the increasing temperature gradient are not nearly as large and as strong as those of the decreasing gradient. Also, even if the upper troposphere effect is comparable to that of the lower troposphere, the sign of the lower level temperature gradient would still likely be dominant as suggested by Held and O'Brien (1992), who show that the eddy heat flux is more sensitive to the lower than to the upper-level mean temperature gradient for equal values of vertical wind shear in an idealized quasigeostrophic model.

Another prominent feature from Fig. 8 is that the magnitude of warming over the continents is much larger than the warming over the oceans. As a result of this, the direct thermal contrast between the oceans and the continents is reduced, an effect considered by Sutcliffe (1951) as a primary reason for the existence of the troughs to the east of the American and Asian continents. The direct thermal effect of the land and sea is of great significance to the differences between the summer and winter flow patterns near the east coasts of the two continents and the associated cyclone-scale disturbances downstream. The weakening of the thermal contrast will shift the coastal circulations toward its summer counterpart and thus tend to reduce the intensity of the troughs and the activity of the eddies.

On the other hand, depending on the magnitude of the reduction in coastal temperature gradient, the coastal cyclogenesis and cyclone activity will possibly become weaker due to less generation of vorticity. This is because the vortex tube stretching is one of the most important mechanisms of generating vorticity in the coastal area during the formation of a cyclone. The generation by the stretching will become less effective with the decrease of the coastal thermal contrast. Cyclones that would have formed under the normal condition will, in the warming case, either not form at all or will form with less intensity depending on the reduction of the temperature gradient. The reduction in coastal thermal contrast also directly decreases the local baroclinicity in the coastal regions, which produces a less favorable condition for cyclongenesis and development. This effect plus the effect of the stretching mechanism can greatly affect the total number and intensity of cyclone events because the east coastal regions of the two continents are the two major regions of cyclogenesis in the Northern Hemisphere (Petterssen, 1956; Whittaker and Horn, 1982). The reduction of cyclone numbers in the three major cyclongenesis regions in Fig. 4 (b) suggests that this is what actually happened in the model simulation.

Another very important factor related to the eddy activity under the greenhouse warming condition that has been suggested by Held (1993) is the global water vapor budget. Water vapor is

the major absorber in the infrared contributing to the greenhouse effect. Its residence time in the atmosphere is on the order of a week and is controlled by convective, radiative and dynamical processes in the atmosphere, and the changes in moisture content will affect the sources and sinks of latent heat which will in turn affect the activity of cyclones and anticyclones (Danard, 1964; Chen and Dell'Osso, 1987).

The increase in specific humidity between the warming and control simulations, similar to those from Washington and Meehl (1984) and others, indicates that the maximum value is around 2 g kg^{-1} in the tropical-to-subtropical lower troposphere. The increase in moisture content is known to have the effect of enhancing the eddy activity. This is because the increase in moisture will increase the latent heat release in the warm sector of the baroclinic disturbance, and thus enhance the transfer of available potential energy into kinetic energy as the warm air rises and moves poleward and the cold air sinks and moves equatorward. The increased moisture content will produce a more favorable environment to generate more kinetic energy and thus intensify the eddy activity.

However, the increase in moisture content in the atmosphere has a different, but potentially more powerful, effect on the eddy activity. Since the increase in moisture content is more abundant in the low latitudes, the meridional eddy latent heat flux increases significantly under the warming condition. Plotted in Fig. 10 is the zonally averaged vertically integrated eddy flux of latent heat of water vapor from both simulations. Although cyclone-scale eddies are less active in the warming condition as indicated in the previous analysis, the eddy latent heat flux increases on average by about 0.4×10^{15} W around 30°N to 50°N. The part that contributed by the cyclone-scale eddies (2.5-6 days) is about 0.2×10^{15} W. The reason for the increase most likely is due to the increase in moisture content under the warming condition, with more moisture in the subtropical air is transferred by the eddies to higher latitudes where the temperature is relatively lower; the air thus becomes saturated, which results in more latent heat release. This is supported by the commonly known results of the increase in extratropical precipitation in warming conditions from other GCMs (Mitchell et al., 1990) and this model. As mentioned before, it is the balance between the equator-to-pole heating gradient and eddy heat flux that determines the meridional temperature gradient and the strength of the eddies. The increase in meridional eddy latent heat flux has two effects: first, it will reduce the meridional temperature gradient more than in the normal condition

when less water vapor is transferred from the low latitudes; second, with the addition of more latent heat transport, the eddies become more efficient in transporting energy poleward. On a global average, fewer and less intense eddies are then required to maintain the same (if not smaller) meridional temperature gradient. It is thus anticipated that the activity of cyclones and anticyclones will decrease as the moisture content increases under the warming condition.

Of the two opposing effects of the water vapor on the cyclone-scale eddy activity, the former is more important for mesoscale and small scale disturbances. This is because moist dynamics tend

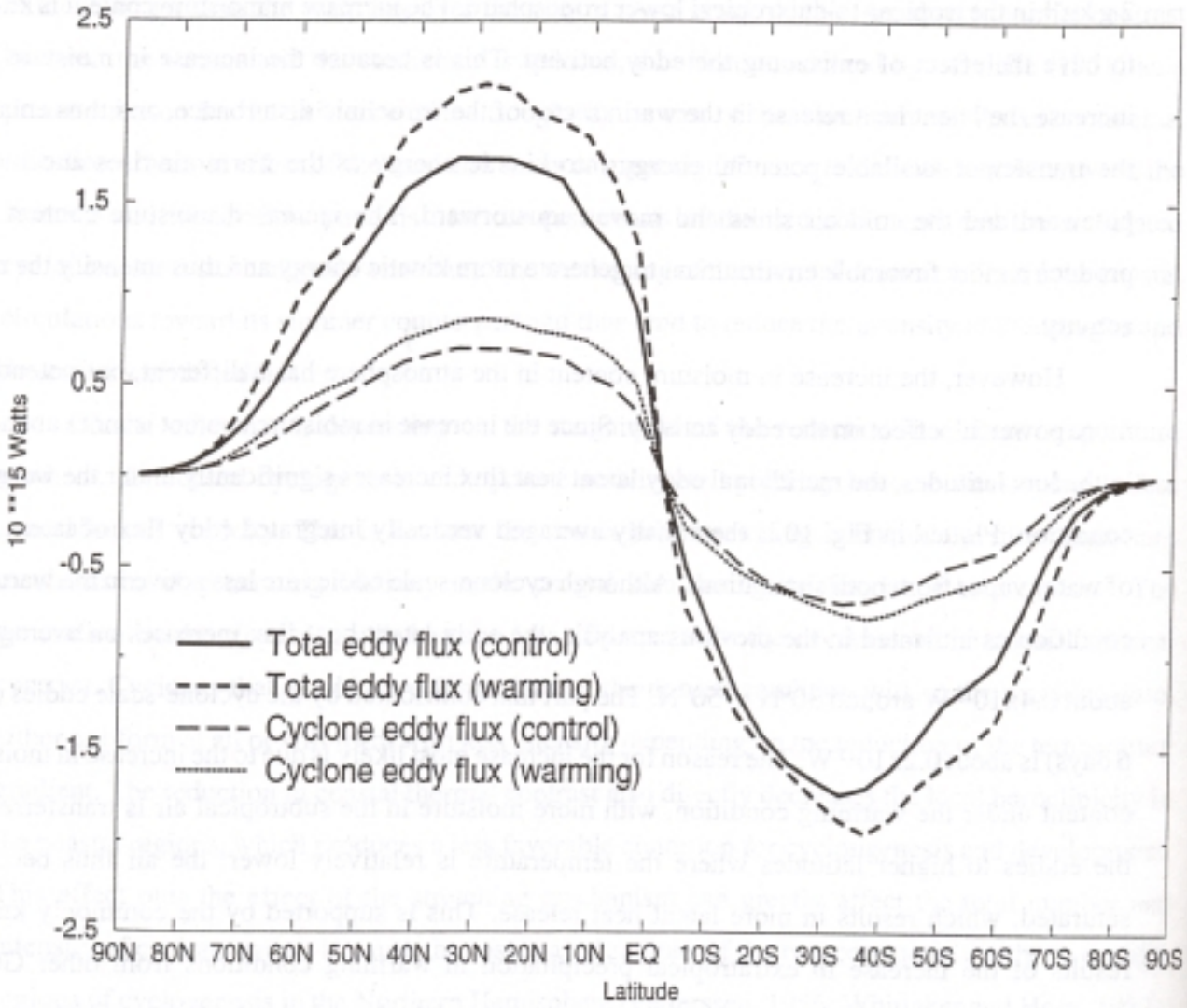

Fig. 10. Winter seasonal averaged mean meridional eddy flux of latent heat from the control and warming simulations. Unit: 10^{15} Watts.

to influence small scale phenomena much more than the large-scale ones. On a planetary scale, the cyclone-scale eddies will be more affected by the latter. Therefore, we believe that the increase in

the moisture content will weaken the extratropical eddy activity.

5. Conclusions and discussion

The objectives of this study, as stated in the introduction, are to investigate the possible changes of cyclone and anticyclone activity under a greenhouse warming scenario. The following conclusions are reached:

(1) The analysis of model simulated variables has indicated that the cyclone and anticyclone activity decreases under greenhouse warming scenario. This decrease is not only reflected in the surface cyclone and anticyclone frequency and the band-passed RMS of 500 hPa geopotential height, but is also discernible from the Eady growth rate maximum.

(2) Three different physical mechanisms contributed to the decreasing eddy activity: a) the decrease of the extratropical lower-to-middle troposphere meridional temperature gradient; b) the reduction of the land-sea thermal contrast in the east coastal regions of the continents; and c) the increase in eddy meridional latent heat fluxes.

Although this study indicates that cyclone-scale eddies become less active in a greenhouse warming climate in NCAR CCM1, the current analysis is far from complete and further studies are warranted.

First, all the conclusions are derived from the ten-year winter seasonal averaged quantities. This decision was made mainly based on the length of the available observed data and the length of the model simulations. The ten-year duration seems to be long enough to have fairly stable statistics of most variables, such as temperature, wind and surface cyclone frequency. To be cautious, comparisons between ten-year and thirty-year averaging were made on selected model simulated quantities. The comparisons indicate that the span of ten years produce the same results as those of the thirty years. Ten years of observational data and model output have been used to study extratropical eddy activity and storm tracks by other investigators as well (Hoskins and Valdes, 1990; Trenberth, 1991).

Second, a complete and satisfactory discussion of the physical mechanisms that caused the decreasing of eddy activity under the warming condition would not be achieved without the examination of the effect of the Hadley circulation, given that a change in the tropical heating structure could change the intensity of the Hadley circulation and thus may greatly affect the

subtropical jet and the extratropical baroclinic wave activity (Chang, 1995). According to Lindzen (1990), the mass flux in the tropical convective clouds increases with warming, and the increase in the mass flux will intensify the strength of the rising branch of the Hadley cell. If this is true, the subtropical high will be intensified along with the baroclinicity and the subtropical jet stream. Depending on the magnitude of the intensification, the effect of the Hadley cell on the eddies could partly offset the effect of decreasing eddy activity.

The mean meridional streamfunction from the control and warming simulations was computed and the maximum magnitude at the center of the Hadley cell was found to decrease by 16×10^9 kg s^{-1} (less than ten percent) under the warming scenario. Del Genio et al. (1991) have indicated that the strength of the Hadley cell increases or decreases slightly depending on the version of the NASA/GISS model used. The most updated version of the NASA/GISS GCM shows a slight decrease in the Hadley cell intensity (Del Genio 1995, personal communication). Based on the results of the current model and those of the NASA/GISS model, the change in the intensity of the Hadley cell under the greenhouse warming scenario seems too small to have any significant effect on the extratropical cyclones and anticyclones. Clearly, this is a problem that needs to be further investigated.

Third, we must bear in mind that all our results are based on model equilibrium simulations. In reality, the concentration of greenhouse gases increases gradually and the climate responds slowly to the gradual changes of greenhouse gas concentrations. The thermal capacity of the oceans will delay and effectively reduce the climatic response to the increased greenhouse gases. To make reliable predictions of climate change under realistic scenarios of increasing forcing by the increase of greenhouse gases, coupled atmosphere-ocean general circulation models are essential. Due to the computational constraint, only a few groups of researchers (Stouffer et al., 1989; Washington and Meehl, 1989; Mitchell et al., 1995; Hasselmann et al., 1995) have performed transient simulations using fully coupled ocean-atmospheric models. The planetary response patterns for both temperature and precipitation of these coupled ocean-atmosphere models for a steadily increasing forcing generally resemble those of an equilibrium simulation, except that the increases are uniformly reduced in magnitude. In rough terms, the temperature response of these time-dependent simulations is about 60% of the current equilibrium simulation. Taking this into consideration, the present conclusions concerning the changing eddy activity will be affected quantitatively, not qualitatively. All of the physical mechanisms discussed in the last section are

still valid for the coupled ocean-atmosphere simulations except the magnitudes of the changes will be smaller. Therefore, there still will be less active extratropical cyclone-scale eddies under the greenhouse warming scenario, but the magnitude of the decrease will be less than that estimated from the equilibrium simulations.

Finally, all the results discussed here are based on simulations from one model. In general, the model simulated results from the control or the perturbed runs are a combination of real climate change which is physically caused and changes due to errors that are inherently related to a specific model. The model dependent uncertainties must be smaller than the real climate change if the model result is to be given credibility. It is very difficult to distinguish the real changes and model dependent uncertainties in a quantitative way. The response of model results to a perturbation has been shown to depend on the control climate (Mitchell et al., 1987). Before the model is used to study this problem, the variables related to the cyclone-scale eddies from the control simulation have been thoroughly evaluated against observations (Zhang, 1995). These model simulated variables, which include surface cyclones and anticyclones and the band-passed RMS of 500 hPa geopotential height, are in general agreement with the observations. However, a model indicating a good control simulation is not sufficient to guarantee that the perturbed runs will be equally well simulated unless the relevant physical mechanisms can be identified. During this study, the relevant physical mechanisms related to the changing eddy activity have been discussed, and the physical interpretations are consistent with results that derived from the model variables. Therefore, it can be stated with confidence that the conclusions about the changing cyclone-scale eddy activity under the greenhouse warming scenario, based on the current understanding of the climate modeling and observations, should be reproduced in most other current generation climate models. We thus conclude that the northern winter extratropical cyclones and anticyclones will become less active in a global warming scenario.

Acknowledgments. This paper is based on a portion of the first author's Ph.D thesis, completed under the second author's supervision at the State University of New York at Albany. We are indebted to W. Lawrence Gates for his valuable suggestions and a thorough review of an earlier draft. Comments and suggestions from James Boyle and Kenneth Sperber are greatly appreciated. James Boyle also provided the data for Figure 3. We wish to thank Anthony D. Del Genio for sharing some results from the NASA/GISS model and constructive discussions. Michael Fiorino,

Peter Gleckler and Anna McCravy helped with Framemaker and some of the figures. This work was supported by the Environmental Science Division of the US Department of Energy under contract DEFG-0292-ER-61369 and the Climate Dynamics Division of the National Science Foundation under contract ATM-9415336.

References

Bates, G. T., and G. A., Meehl, 1985: The effects of CO_2 concentration on the frequency of blocking in a general circulation model coupled to a simple mixed layer ocean model. *Mon. Wea. Rev.*, **114,** 687-701.

Chang, E. K. M., 1995: The influence of Hadley Circulation intensity changes on extratropical climate in an idealized model. *J. Atmos. Sci.*, **52,** 2006-2024.

Chen, S.-J., and L. Dell'Osso, 1987: A numerical case study of East Asian coastal cyclogenesis. *Mon. Wea. Rev.*, **115,** 477-487.

Darnard, M. B., 1964: On the influence of released latent heat on cyclone development. *J. Appl. Meteo.*, **3**, 27-37.

Del Genio, A. D., A. A. Lacis, and R. A. Ruedy, 1991: Simulations of the effect of a warmer climate on atmospheric humidity. *Nature*, **351**, 382-385.

Giorgi, F., 1990: Simulation of regional climate using a limited area model nested in a general circulation model. *J. Climate.* **3**, 941-963.

Hasselmann, K., Bengtsson, L., Cubasch, U., Hegerl, G.C., Rodhe, H., Roeckner, E., Storch, H.v., Voss, R. & Waszkewitz, 1995: Detection of anthropogenic climate changes using a fingerprint method. *Max-Planck-Institue fur Meteorologie,* Report No. **168**, Hamburg, Germany, 20 pp.

Held, I. M., 1993: Large-scale dynamics and global warming. *Bull. Amer. Meteor. Soc.*, **74**, 228-241.

Held, I. M., and E. O'Brien, 1992: Quasigeostrophic turbulence in a three-layer model: Effects of vertical structure in the mean shear. *J. Atmos. Sci.*, **49,** 1861-1870.

Holopainen, E. O., 1965:. On the role of mean meridional circulations in the energy balance of the atmosphere. *Tellus,* **17**, 285-294.

Hoskins, B. J., and P. J., Valdes, 1990: On the existence of storm-tracks. *J. Atmos. Sci.*, **47**, 1854-1864.

Houghton, J. T., G. J. Jenkins, and J. J. Ephraums, (eds) 1990: *Climate Change, The IPCC Scientific Assessment.* Cambridge Univ. Press, 364pp.

Houghton, J. T., B. A. Callander and S. K. Varney (eds), 1992: *Climate Change, The Supplementary Report to the IPCC Scientific Assessment.* Cambridge Univ. Press, 200pp.

Kiehl, J., and D. Williamson, 1991: Dependence of cloud amount on horizontal resolution in the

National Center for Atmospheric Research community climate model. *J. Geophy. Res.*, **96,** 10955-10980.

Klein, W.H.,1957: The frequency of cyclones and anticyclones in relation to the mean circulation. *J. Meteor.*, **15,** 98-102.

Konig, W., R. Sausen, and F. Sielmann, 1993: Objective identification of cyclones in GCM simulations. *J. Climate,* **6,** 2217-2231.

Lambert, S. J., 1988: A cyclone climatology of the Canadian Climate Centre general circulation model. *J. Climate*, **1,** 109-115.

Lambert, S. J., 1995: The effect of enhanced greenhouse warming on winter cyclone frequencies and strengths. *J. Climate*, **8**, 1447-1452.

Lindzen, R. S., 1990: Some coolness concerning global warming. *Bull. Amer. Meteor. Soc.*, **71**, 288-299.

Lindzen, R.S., and B. Farrell, 1980: A simple approximate result for the maximum growth rate of baroclinic instabilities. *J. Atmos. Sci.*, **37**, 1648-1654.

Mitchell, J. B., C. A. Wilson, and W. M. Cunnington, 1987: On CO_2 climate sensitivity and model dependence of results. *Quart. J. Roy. Meteor. Soc.*, **113**, 293-322.

Mitchell, J. B., S. Manabe, T. Tokioka and V. Meleshko, 1990: Equilibrium climate change. *Climate Change. The IPCC Scientific Assessment.* 364pp.

Mitchell, J. B., T. C. Johns, J. M. Gregory, and S. F. B. Tett, 1995: Climate response to increasing levels of greenhouse gases and sulphate aerosols. *Nature,* **376**, 501-504.

Newton, C., 1969: The role of extratropical disturbances in the global atmosphere. *The Global Circulation of the Atmosphere.* Roy. Meteor. Soc., 137-158, London, 257pp.

Newton, C., and E. O. Holopainen, 1990: *The Erik Palmen Memorial Volume.* Amer. Meteor. Soc., Boston, 262pp.

Petterssen, S., 1956: *Weather Analysis and Forecasting.* Vol. 1. 2nd ed., McGraw- Hill, New York, 422 pp.

Stouffer, R. J., S. Manabe, and K. Bryan, 1989: Interhemispheric asymmetry in climate response to a gradual increase of atmospheric carbon dioxide. *Nature*, **342**, 660- 662.

Sutcliffe, R. C., 1951: Mean upper contour patterns of the Northern Hemisphere-the thermal-synoptic viewpoint. *Quart. J. Roy. Meteor. Soc.*, **77**, 435-440.

Trenberth, K. E., 1991: Storm tracks in the Southern Hemisphere. *J Atmos. Sci.*, **48**, 2159-2178.

Wang, W-C., M. P. Dudek, X.-Z. Liang, and J. T. Kiehl, 1991: Inadequacy of effective CO_2 as a proxy in simulating the greenhouse effect of other radiatively active gases. *Nature*, **350**, 573-577.

Wang, W-C., M.P. Dudek, and X.-Z. Liang, 1992: Inadequacy of effective CO_2 as a proxy in assessing the regional climate change due to other radiatively active gases. *Geophys. Res. Lett.*, **19**, 1375-1378.

Washington, W.M., and G. A. Meehl, 1984: Seasonal cycle experiment on the climate sensitivity due to a doubling of CO_2 with an atmospheric general circulation model coupled to a simple mixed-layer ocean model. *J. Geophs. Res.*, **89**, 9475-9503.

Washington, W.M., and G. A. Meehl, 1989: Climate sensitivity due to increased CO_2: Experiments with a coupled atmosphere and ocean general circulation model. *Climate. Dyn.*, **4**, 1-38.

Whittaker, L.M., and L.H. Horn, 1981: Geographical and seasonal distribution of North America cyclogenesis. 1958-1977. *Mon Wea. Rev.*, **109**, 2312-2322.

Whittaker, L.M., and L.H. Horn, 1982: Atlas of Northern Hemisphere extratropical cyclone activity, 1958 - 1977. *Research Report of Univ. of Wisconsin - Madison.*

Williamson, D.L., J. T. Kiehl, V. Ramanathan, R. E. Dickinson, and J. Hack, 1987: Description of NCAR community climate model (CCM1). *NCAR Technical Note.* NCAR/TN- 285+STR, Boulder, Colorado.

Zhang, Y., 1995: Extratropical cyclone-scale eddies simulated from a climate model. Ph.D dissertation, State University of New York at Albany. 161pp.

Zishka, K.M., and P.J. Smith, 1980: The climatology of cyclones and anticyclones over North America and surrounding ocean environs for January and July, 1950-77. *Mon. Wea. Rev.*, **108**, 387-401.